QUANTITATIVE MINERAL ANALYSIS BY FOURIER TRANSFORM INFRARED SPECTROSCOPY

Abigail Matteson and Michael M. Herron

Schlumberger-Doll Research
Old Quarry Road, Ridgefield, Ct. 06877-4108

ABSTRACT

This paper presents a methodology for obtaining quantitative mineral concentrations from transmission Fourier Transform Infrared (FTIR) spectroscopy. The procedure results in absorbance spectra that are reproducible to within ±5% relative standard deviation. A set of 49 mixtures composed of quartz, opal-A, orthoclase, oligoclase, calcite, dolomite, kaolinite, illite, smectite, chlorite, biotite, muscovite, glauconite and pyrite was constructed to test the methodology. The relative concentrations of the minerals correspond to levels commonly found in clastic and carbonate lithologies. The sample spectra were evaluated using whole-spectrum least-squares spectral processing, which produced an average absolute difference between the known and derived mineral concentrations of ±2.6 wt %. When whole-spectrum nonnegative least-squares processing was applied to the spectra, the error between known and derived mineral concentrations was reduced to ±1.2 wt %. This technique does not require a size separation step to assess the weight percent of illite, smectite, kaolinite and chlorite in a sample. The accurate FTIR methodology is applicable to whole core, sidewall and outcrop samples. Although only a 1.0 mg sample split is analyzed, a larger initial sample size (e.g., 4 g in this study) ensures that the mineralogy is representative of the formation composition.

INTRODUCTION

A fundamental component of sedimentary formation description is mineralogy. Our ability to measure sedimentary mineral assemblages, especially when clay minerals are present, is generally regarded as semi-quantitative.[1] This is because X-ray diffraction (XRD), the prevalent methodology for identifying minerals, has some inherent problems in quantitative analysis mostly due to particle size and uncontrolled orientation effects coupled with natural variability in mineral diffraction spectra. The common practice of fines separation to enhance clay mineral identification introduces additional error since not all clay minerals are finer than the usual 2 μm cutoff.

Fourier transform infrared (FTIR) spectroscopy is an alternative method for acquiring quantitative mineralogy. The mineralogy of a mixture can be extracted from its FTIR spectrum because minerals exhibit most of their fundamental molecular vibration modes in the mid-

infrared (4000 to 400 cm^{-1})[2-5] and the absorbance bands of each component in the mixture are proportional to the pure mineral spectrum.[6-12] The latter is known as Beer's Law:

$$A = \sum_{i=1}^{n} \varepsilon_i \, l \, c_i \qquad (1)$$

where A is the absorbance of a band, ε_i is the absorptivity of component i, l is the absorption path length (pellet thickness), and c_i is the concentration of component i. To obtain accurate mineralogy from FTIR transmission spectroscopy, we developed a set of experimental and data collection procedures. We tested these procedures on a set of mineral assemblages, which mimic the mineralogy typical of sedimentary lithologies.

EXPERIMENTAL METHODS

A suite of clastic and carbonate mixtures was designed based on mineral combinations common to many sedimentary environments. Examples of clean and shaley sands as well as mudstones, carbonates and diatomites were accounted for. Fourteen minerals were chosen to make up the mineral mixtures: quartz, opal-A, orthoclase, oligoclase, calcite, dolomite, kaolinite, illite, smectite, chlorite, biotite, muscovite, glauconite, and pyrite. Each mineral in the mixture set was distributed within concentration ranges typical of sedimentary rocks. There are a total of 49 mixtures of which 28 are original and 21 are repeats.

The mixture minerals were selected from a library of standards that were characterized by FTIR spectroscopy, X-ray diffraction (XRD) and chemistry. Chemical analyses, which include neutron activation, induction coupled plasma spectroscopy and fluorescence spectroscopy, were performed by X-Ray Assay Laboratories. Four additional standards were included in the mixtures to account for chemical and/or structural variability within a mineral. The calcite species include calcite and calc-spar (CAL1 and CAL2). Kaolinite mineral species, KAO1 and KAO2, have Hinkley Indices of 0.6 and 1.5 as determined from X-ray diffraction indicating low and high degrees of crystallographic order. In the mixtures high (2.5% Fe^{+2}) and low (0.8% Fe^{+2}) iron smectites, SM1 and SM2, are represented as well as high (10%) and low (3%) magnesium chlorites, CHL1 and CHL2. Table 1 lists the mineral standards, mineral abbreviations adopted in this paper and their locations.

Sample Preparation and Data Collection Procedures

Four grams of each mixture were prepared by first grinding the constituent minerals to less 500 μm and then weighing the material to within ±0.3 mg of the preordained amounts. To ensure that the minerals were well mixed, the dry material was placed in 50 milliliters of alcohol and the slurry was agitated with a magnetic stir bar for five minutes then decanted into a petri dish and dried in an oven (80°C) for twenty-four hours. The mixture was then hand mixed with a mortar and subsequently split with a sample splitter; an aliquot was reserved for FTIR analyses.

The alkali halide (KBr) pressed pellet method for sample preparation was adopted. To minimize the dispersion of the IR beam and distribute the sample homogeneously in the carrier it is

essential that the grain size of the sample be less than 2.5 μm (4000 cm^{-1}).[6] This optimum grain size was obtained by grinding the sample in a micronizing mill. A sample to KBr ratio was chosen to ensure that absorbance bands were in the linear region of Beer's law and that the signal-to-noise ratio was maximized. The sample and KBr were weighed on a microbalance and then combined using an automatic mixer. The mixtures of sample and KBr were evacuated prior to pressing at 12,000 psi for 10 minutes, under vacuum, to produce 13 X 0.55 mm pellets.

Transmission FTIR spectra were collected with a Perkin Elmer 1760X spectrometer. The sample chamber was purged with purified compressed air to remove water vapor and CO_2 prior to scanning the pellet. The spectra were collected over the 4000 to 400 cm^{-1} frequency range, at a resolution of 4 cm^{-1}, by performing a series of interleaved sample and background scans. The transmittance spectra were then converted to absorbance spectra.

RESULTS AND DISCUSSION

The success of obtaining accurate mineralogy from FTIR spectroscopy depends on several factors: 1) that analytical procedures minimize variance between spectra of the same mineral; 2) that the FTIR spectra of different mineral standards are distinguishable from one another; 3) that chemical or structural variability within a mineral be accounted for; 4) that the observed FTIR spectrum is a linear combination of the standard spectra; and 5) that appropriate spectral processing programs are implemented. In the following section we will report experimental errors and how they were minimized, review the FTIR spectra of the mixture minerals, compare two full-spectrum processing programs and present the results for the mineral mixtures.

Experimental Error

Analytical errors were calculated by measuring the relative standard deviation (RSD) of the maximum absorbance peak (three spectra per sample) for each standard and one mixture (Table 2). Analytical error was reduced when the task of mixing the sample with the KBr was carried out by an automated mixer; this procedure more effectively dispersed the sample in the KBr than did conventional hand mixing. The smectite spectra exhibited the most dramatic improvement; the absorbance of the Si-O stretch peak (100 to 1200 cm^{-1}) increased by a factor of three and the relative standard deviation of this peak declined from 15 to 3% when the sample and KBr were combined with an auto-mixer (Fig. 1).

The absorbance spectra of the mixtures exhibit two additional sources of error. The first occurs between 2800 and 3000 cm^{-1} and corresponds to the C-H stretching vibrations of the hydrocarbon film that remains on the sample after it has been ground in alcohol. The second and third occur between 1630 and 1730 cm^{-1} and 3200 to 3400 cm^{-1} and are thought to be associated with water that is adsorbed on the fine-grained sample material.[3] Because it is difficult to control the occurrence of the impurities, we exclude the 2800 to 3000 cm^{-1} region of the spectrum from further analysis. The adsorbed water regions are not blanked out because they overlap either with the carbonates or with the adsorbed/interlayer water of some of the clays. Instead a spectrum of a KBr pellet, which was prepared in the same fashion as sample and KBr pellets were, is included in the analysis to account for the adsorbed water regions.

Mineral Standard Spectra

The mineral standards in this set of mixtures can be divided into four major groups: the tectosilicates (framework silicates, e.g., quartz), phyllosilicates (layer silicates, e.g., clays), the carbonates, and one sulfide (pyrite). The mineral groups have FTIR absorbance band features that make them clearly different from one another. However, within each group the spectra are similar. The absorbance spectra of the twenty mineral standards are plotted in Fig. 2.

The silicate spectra are characterized by Si-O stretching and bending vibrations between 1200 and 800 cm^{-1} and 600 to 400 cm^{-1}. The phyllosilicates can be separated from the tectosilicates based on the occurrence of the O-H stretch vibrations at 3750 to 3400 cm^{-1}. The carbonates are characterized by strong absorption bands due to internal vibrational modes of the CO_3^{-2} groups, which occur between 1500 and 1400 cm^{-1}. The covalent Fe-S bonding in pyrite gives rise to an absorbance band near the edge of the mid-infrared (around 400 cm^{-1}); this opaque and specular mineral also exhibits characteristic light scattering.

Correlation coefficients for the mineral standard FTIR spectra, Table 3, demonstrate the co-linearity of the spectra within mineral groups. Of the tectosilicate mineral standards two pairs of minerals have correlation coefficients greater than 0.97, quartz and opal-A, and orthoclase and oligoclase. The calcite and dolomite spectra are similar with a correlation coefficient of 0.91. Of the phyllosilicates, the smectite, illite and glauconite spectra are most visually similar to one another and to the micas: biotite and muscovite (Fig. 2); the correlation coefficients for these minerals are all greater than 0.9. The mineral species spectra are even more highly correlated; calcite and calc-spar correlate at 0.999, the two chlorite species correlate at 0.990 and the kaolinite species correlate at 0.993 where the only visual differences between the kaolinite spectra are slight changes in relative peak intensities in the O-H stretch region. The FTIR spectrum of pyrite does not correlate with any of the other mineral spectra.

Spectral Processing Procedures

The analytical procedures followed in this study ensure that absorbance bands are in the linear region of Beer's law (Eq. 1) and that the path length and absorptivity coefficients are constant. Therefore, each mixture spectrum is a linear combination of the mineral standard spectra multiplied by the concentration of each mineral standard in the mixture. Two standard full spectrum processing programs, least squares (LS) and nonnegative least squares (NNLS), were run to solve for the mineralogy of the mixtures. The concentrations are determined from minimizing the difference between the measured FTIR spectrum and the product of the spectra and the concentrations of mineral standards over the mid-infrared. For the LS program there are no constraints on the solution while for the NNLS program the solution vector is constrained to be greater than zero.

The mineralogy results derived from LS and NNLS programs are plotted against known mineral concentrations in Fig. 3. The error, the average absolute difference for the 14 standards in the mixtures, is ±2.6 and ±1.2 wt % for the LS and NNLS results, respectively. For mineral pairs with highly correlated spectra the LS solution occasionally produces compensating negative and positive concentrations. An example is mixture 0591, which contains no illite or smectite. For this sample the LS solution found -14 wt % illite and 10 wt % smectite. This physically

unrealistic solution is avoided in the NNLS program, which found, no illite or smectite. All subsequent results reported in this paper will be from the NNLS program.

FTIR Mineralogy

The FTIR mineralogy results for each mineral are plotted in Figs. 4 and 5 where the mineralogy determined from FTIR spectroscopy (solid line) is compared to known mineral concentrations (solid circles) for all samples in the mixture set. The non-phyllosilicate results are given in Fig. 4 and the phyllosilicate results are shown in Fig. 5. The average absolute difference between measured and derived concentrations is calculated for each mineral (zeros are included in the average) and is printed on the plots.

The agreement between the FTIR-derived and the known concentrations of tectosilicate (quartz, opal-A, oligoclase and orthoclase) and carbonates (calcite and dolomite) is very good with an average absolute difference below ±1.6 wt %. It is clear from the results that quartz can be accurately separated from opal-A; this separation is impossible with XRD because of the amorphous structure of opal-A. In wells where quartz and opal-A occur concurrently, such as in the Monterey formation, it is essential to differentiate these two silicate phases because these minerals have nearly identical compositions (SiO_2 and $SiO_2 \cdot n\ H_2O$) but very different grain densities (2.65 and 1.9). Therefore, large errors in log porosity may occur. Accurate feldspar mineralogy is essential since they are common in arenaceous sediments.

The correlation coefficients for the FTIR spectra: illite, smectite, kaolinite, chlorite, biotite and muscovite suggest that it might be difficult to differentiate these minerals from one another (Table 2). Fig. 5 demonstrates that each of the four clay types can be quantified and on average the clays can be distinguished from the micas. When a mixture contains illite, smectite, chlorite and glauconite, the agreement between measured and predicted phyllosilicates is slightly worse than for other phyllosilicate combinations.

Mineral Species

It has been demonstrated that FTIR spectroscopy can be used to quantify the mineralogy of a complex mixture but can this method distinguish between mineral species where only slight differences in structure or chemistry exist between standards of the same mineral? The mineralogy results for the mineral species are shown in Fig. 6 where the FTIR spectroscopy mineralogy is plotted against the known mineral concentrations.

The degree of similarity between the mineral species spectra indicates that it might be difficult to determine species' mineralogy. The agreement between measured and known carbonate species, CAL1 and CAL2, is poor and leads to the conclusion that it is difficult to differentiate between calcite and calc-spar. On the other hand the FTIR-derived concentrations of high and low iron smectite (SM1 and SM2), low and high crystalline kaolinite (KAO1 and KAO2), and high and low magnesium chlorite (CHL1 and CHL2) are in fairly good agreement with the known mineral concentrations. However, for each mineral the agreement between derived and known mineralogy is better when the sum of the species are compared rather than when the individual species are evaluated.

CONCLUSIONS

A set of mineral mixtures was prepared to test laboratory quantitative mineralogy methods. The assemblages were designed to reflect the mineralogy of a range of sedimentary environments. These complex mixtures of minerals constitute a rigorous test for any experimental mineralogy procedure; in this study the FTIR spectroscopy (transmission) approach was evaluated. The issue of natural variability within a mineral, e.g. different chemical and structural states or diagenetic and stress history, was also addressed to a limited extent by including mineral species in the mixtures.

A set of analytical and data collection procedures was developed to reduce variance between FTIR spectra of the same sample. For the pressed pellet method of sample preparation, it is essential that the sample be ground to about 2.5 μm, that the sample and carrier (KBr) be weighed with a microbalance and subsequently combined with an auto-mixer, and a vacuum be applied to the mixture before and during pressing. The entire sample is analyzed avoiding errors inherent in the common XRD practice of clay separation. These analytical procedures produced relative standard deviations for the maximum absorbance peak of the mixtures and mineral standards of less than ±5%.

The method of spectral processing is fundamental to determining accurate mineralogy from FTIR spectroscopy. Many minerals in the mixtures have similar structures and/or chemical compositions, which yield highly correlated FTIR spectra. Despite this and the fact that only a small fraction of the mixture (0.125 wt %) is sampled, the average absolute error between derived (LS solution) and known mineralogy for all minerals in the mixtures is ±2.6 wt %. The unrealistic negative mineral concentrations of the LS program are avoided when a NNLS program is run and the error is reduced to ±1.2 wt %. Therefore, with FTIR spectroscopy we were able to quantify the types and amounts of clays, illite, smectite, chlorite and kaolinite; the micas, biotite and muscovite; the carbonates, calcite and dolomite; the silicates, quartz, opal-A and the feldspars; and a sulfide, pyrite.

Natural variance within four minerals was accounted for by including additional mineral species spectra as standards in the mixtures. We solved for each of the individual species and found that for the clays, smectite, chlorite and kaolinite there was a chance to solve for the correct species but that it was nearly impossible to differentiate between calcite and calc-spar. For each mineral the sum of the species gave the best results when compared to known mineral concentrations.

Acknowledgment

We thank M. Supp and G. Gustavson for laboratory measurements.

REFERENCES

1. Moore, D.M. and Reynolds, R.C. *X-Ray Diffraction and the Identification and Analysis of Clay Minerals,* Oxford University Press, New York, (1989), 272-307.

2. Farmer, V.C. (ed.): *The Infrared Spectra of Minerals*, Mineralogical Society, London, (1974).

3. Salisbury, J.W., Walter, L.S., and Vergo, N.: *Mid-Infrared (2.1 - 20.0 μm) Spectra of Minerals*, U.S. Geological Survey, Open File Report, Reston, Virginia (1987).

4. Smith, J.V.: *Feldspar Minerals Crystal Structure and Physical Properties*, Springer-Verlag, New York, (1984), 511-530.

5. Kodama, H.: *Infrared Spectra of Minerals Reference Guide to Identification and Characterization of Minerals for the Study of Soils*, Technical Bulletin 1985-1E, Research Branch, Agriculture Canada, Ottawa, Ontario (1985).

6. Estep-Barnes, P.A.: "Infrared Spectroscopy," in *Physical Methods in Determinative Mineralogy*, J. Zussman (ed.), Academic Press, New York, (1977), 572-574.

7. Liang, K.K., Supp, M., and Murphy, W.F.: "Mapping Mineralogy Distribution and Abundance in Rock Samples by Scanning Fourier Transform Infrared Microscopy," *Scanning* (1990) **12**, 168-178.

8. Harville, D.G. and Freeman, D.L.: "The Benefits and Application of Rapid Mineral Analysis Provided by Fourier Transform Infrared Spectroscopy," paper 18120, presented at the 1988 SPE Annual Technical Conference and Exhibition, Houston, October 2-5.

9. Antoon, M.K., Koenig, J.H., Koenig, J.L.: "Least-Squares Curve-Fitting of Fourier Transform Infrared Spectra with Applications to Polymer Systems," *Applied Spectroscopy* (1977), v. 31, 518-524.

10. Brown, J.M. and Elliott, J.J.: "The Quantitative Analysis of Complex, Multicomponent Mixtures by FT-IR; The Analysis of Minerals and of Interacting Organic Blends," in *Chemical, Biological and Industrial Applications of Infrared Spectroscopy*:, J. During (ed.), Chichester, Wiley, (1985), 111-128.

11. Painter, P.C., Rimmer, S.M., Snyder, R.W., Davis, A., "A Fourier Transform Infrared Study of Mineral Matter in Coal: The Application of a Least Squares Curve-Fitting Program," *Applied Spectroscopy* (1981) v. 35, 102-106.

12. Snyder, R.W., Painter, P.C., Cronauer, D.C., "Development of FT-i.r. Procedures for the Characterization of Oil Shale," Fuel (1983), v. 62, 1205-1214.

Table 1. Mineral Standards

Standard		Location
Quartz	QTZ	Brazil
Opal-A	OPA	Santa Barbara, California
Oligoclase	OLIG	Von Ytterby, Sweden
Orthoclase	ORTH	South Dakota
Kaolinite 1	KAO1	Oneal Pit, Macon, Georgia
Kaolinite 2	KAO2	Wilkinson County, Georgia
Illite	ILL	Fithian, Illinois
Smectite 1	SM1	Crook County, Wyoming
Smectite 2	SM2	Unknown
Chlorite 1	CHL1	Eldorado County, California
Chlorite 2	CHL2	Ishpeming, Michigan
Glauconite	GLA	Birmingham, New Jersey
Biotite	BIO	Bancroft, Ontario
Muscovite	MUS	Stoneham, Maine
Calcite 1	CAL1	Hurley, New Mexico
Calcite 2	CAL2	Dover, England
Dolomite	DOL	Lee, Massachusetts
Pyrite	PYR	Huanzala, Peru

Table 2. Analytical Errors

Standard	Absorbance Band cm^{-1}	Absorbance Mean	Absorbance SD	RSD (%)
Quartz	1085	1.389	0.039	2.8
Opal-A	1099	1.044	0.008	0.7
Oligoclase	1015	0.601	0.002	0.3
Orthoclase	1016	0.680	0.001	0.2
Kaolinite 1	1034	0.758	0.034	4.5
Kaolinite 2	1034	0.730	0.007	0.9
Illite	1030	0.661	0.009	1.4
Smectite 1	1052	0.756	0.037	4.9
Smectite 2	1044	0.632	0.019	3.1
Chlorite 1	984	0.339	0.005	1.5
Chlorite 2	984	0.409	0.020	4.9
Glauconite	1006	0.500	0.014	2.8
Biotite	1026	0.580	0.018	3.0
Muscovite	1001	0.595	0.019	3.1
Calcite 1	1431	1.171	0.015	1.5
Calcite 2	1431	1.278	0.026	2.0
Dolomite	1450	1.269	0.016	1.2
Pyrite	4000	1.278	0.015	1.2
Mix 1591	1033	0.594	0.016	2.6

Table 3. Correlation Coefficients for Mineral Standard FTIR Spectra

	QTZ	OPA	OLIG	ORTH	KAO1	KAO2	ILL	SM1	SM2	CHL1	CHL2	GLA	BIO	MUS	CAL1	CAL2	DOL	PYR
QTZ	1.000	**0.967**	0.676	0.671	0.523	0.507	0.540	0.683	0.793	0.201	0.250	0.525	0.292	0.438	-0.040	-0.037	-0.033	-0.260
OPA	**0.967**	1.000	0.744	0.735	0.595	0.578	0.602	0.735	0.849	0.265	0.312	0.581	0.355	0.504	-0.054	-0.050	-0.044	-0.273
OLIG	0.676	0.744	1.000	**0.973**	0.827	0.803	0.887	0.881	**0.904**	0.564	0.587	0.850	0.695	0.833	-0.055	-0.051	-0.039	-0.332
ORTH	0.671	0.735	**0.973**	1.000	0.823	0.799	0.879	0.847	0.883	0.624	0.651	0.876	0.741	0.853	-0.054	-0.049	-0.038	-0.391
KAO1	0.523	0.595	0.827	0.823	1.000	**0.996**	**0.929**	0.881	0.874	0.673	0.701	0.842	0.723	**0.912**	-0.086	-0.081	-0.068	-0.372
KAO2	0.507	0.578	0.803	0.799	**0.996**	1.000	**0.905**	0.852	0.850	0.647	0.675	0.814	0.704	0.892	-0.081	-0.076	-0.063	-0.371
ILL	0.540	0.602	0.887	0.879	**0.929**	**0.905**	1.000	**0.945**	**0.918**	0.729	0.741	**0.944**	0.829	**0.974**	-0.063	-0.058	-0.046	-0.382
SM1	0.683	0.735	0.881	0.847	0.881	0.852	**0.945**	1.000	**0.973**	0.586	0.606	0.855	0.685	0.870	-0.035	-0.029	-0.021	-0.355
SM2	0.793	0.849	**0.904**	0.883	0.874	0.850	**0.918**	**0.973**	1.000	0.555	0.584	0.843	0.655	0.836	-0.065	-0.060	-0.050	-0.354
CHL1	0.201	0.265	0.564	0.624	0.673	0.647	0.729	0.586	0.555	1.000	**0.990**	0.847	0.897	0.777	-0.087	-0.084	-0.057	-0.368
CHL2	0.250	0.312	0.587	0.651	0.701	0.675	0.741	0.606	0.584	**0.990**	1.000	0.851	0.876	0.788	-0.103	-0.099	-0.070	-0.374
GLA	0.525	0.581	0.850	0.876	0.842	0.814	**0.944**	0.855	0.843	0.847	0.851	1.000	**0.932**	**0.946**	-0.064	-0.060	-0.043	-0.386
BIO	0.292	0.355	0.695	0.741	0.723	0.704	0.829	0.685	0.655	0.897	0.876	**0.932**	1.000	0.869	-0.048	-0.045	-0.022	-0.397
MUS	0.438	0.504	0.833	0.853	**0.912**	0.892	**0.974**	0.870	0.836	0.777	0.788	**0.946**	0.869	1.000	-0.065	-0.061	-0.047	-0.425
CAL1	-0.040	-0.054	-0.055	-0.054	-0.086	-0.081	-0.063	-0.035	-0.065	-0.087	-0.103	-0.064	-0.048	-0.065	1.000	**0.999**	**0.919**	-0.186
CAL2	-0.037	-0.050	-0.051	-0.049	-0.081	-0.076	-0.058	-0.029	-0.060	-0.084	-0.099	-0.060	-0.045	-0.061	**0.999**	1.000	**0.913**	-0.183
DOL	-0.033	-0.044	-0.039	-0.038	-0.068	-0.063	-0.046	-0.021	-0.050	-0.057	-0.070	-0.043	-0.022	-0.047	**0.919**	**0.913**	1.000	-0.194
PYR	-0.260	-0.273	-0.332	-0.391	-0.372	-0.371	-0.382	-0.355	-0.354	-0.368	-0.374	-0.386	-0.397	-0.425	-0.186	-0.183	-0.194	1.000

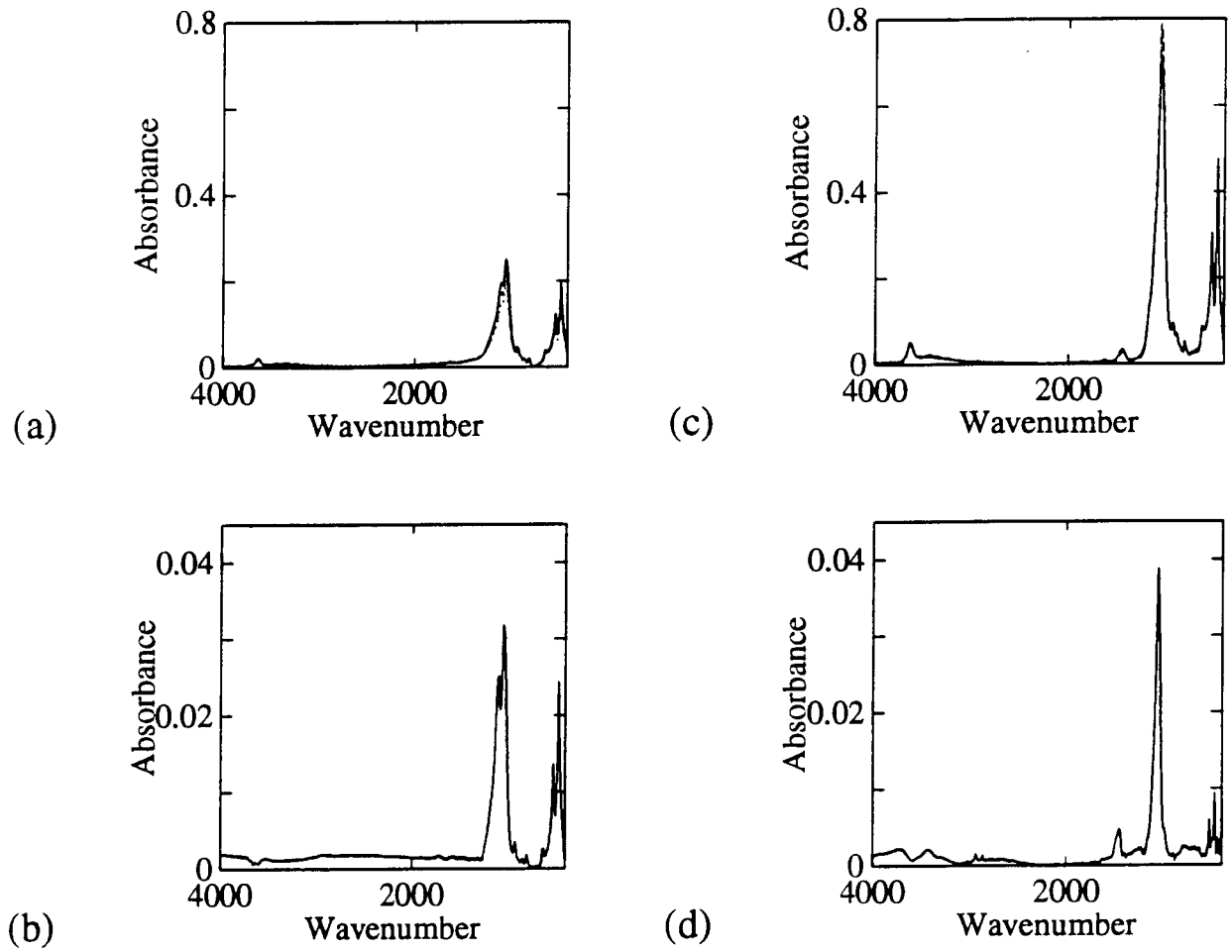

Fig. 1—The FTIR spectra of three hand-mixed smectite and KBr samples (a) and their associated standard deviation (b). Three FTIR spectra of auto-mixed smectite and KBr samples (c) and their associated standard deviation (d).

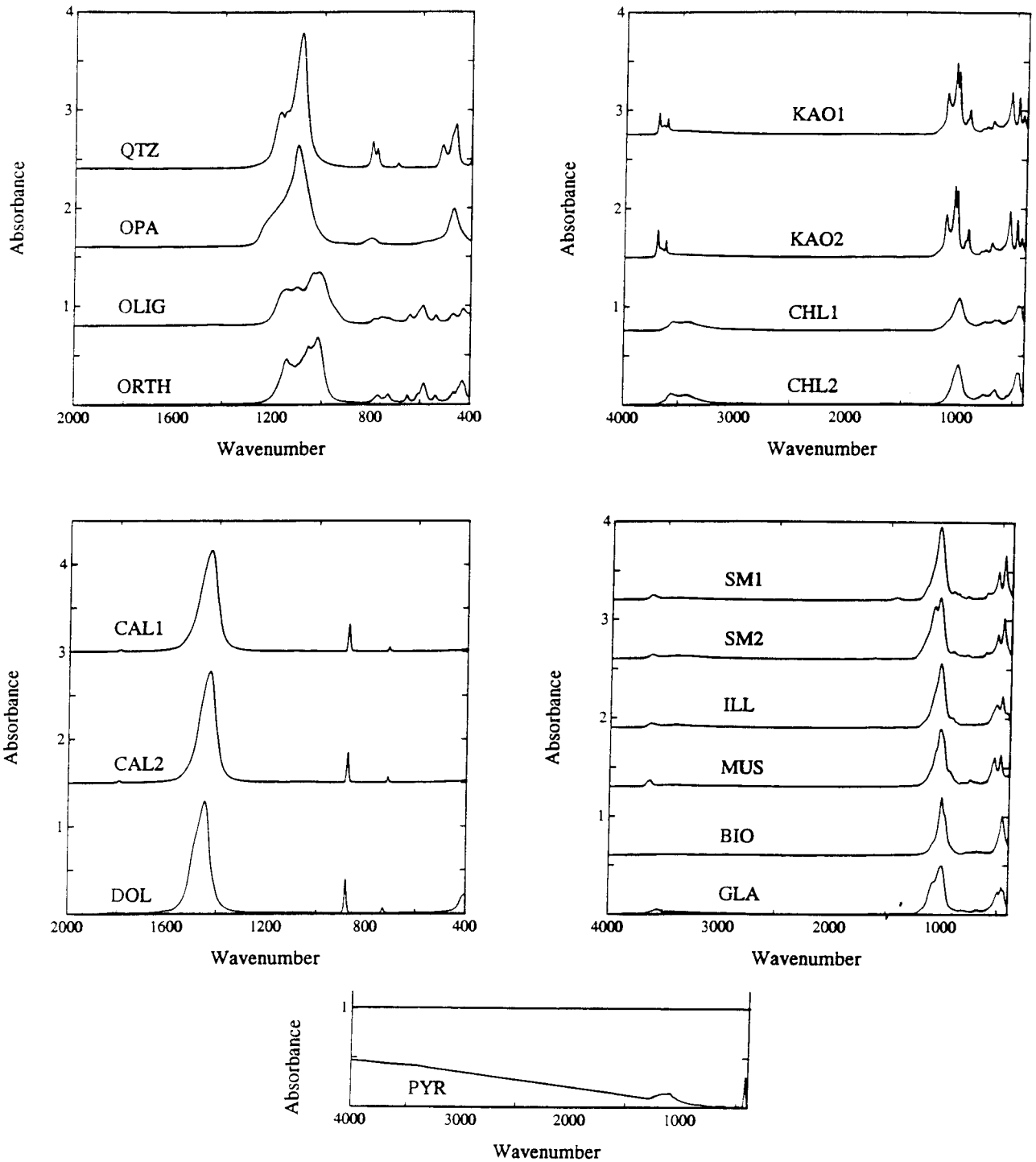

Fig. 2—The FTIR spectra of the tectosilicates (2000 to 400 cm^{-1}): quartz, opal-A, oligoclase, orthoclase; the carbonates: calcites, CAL1 and CAL2, and dolomite; the FTIR spectra of the phyllosilicates (4000 to 400 cm^{-1}): kaolinites, KAO1 and KAO2, and chlorites, CHL1 and CHL2; and smectites, SM1 and SM2, illite, muscovite, biotite and glauconite; and the sulfide, pyrite. The spectra have been offset for visual enhancement.

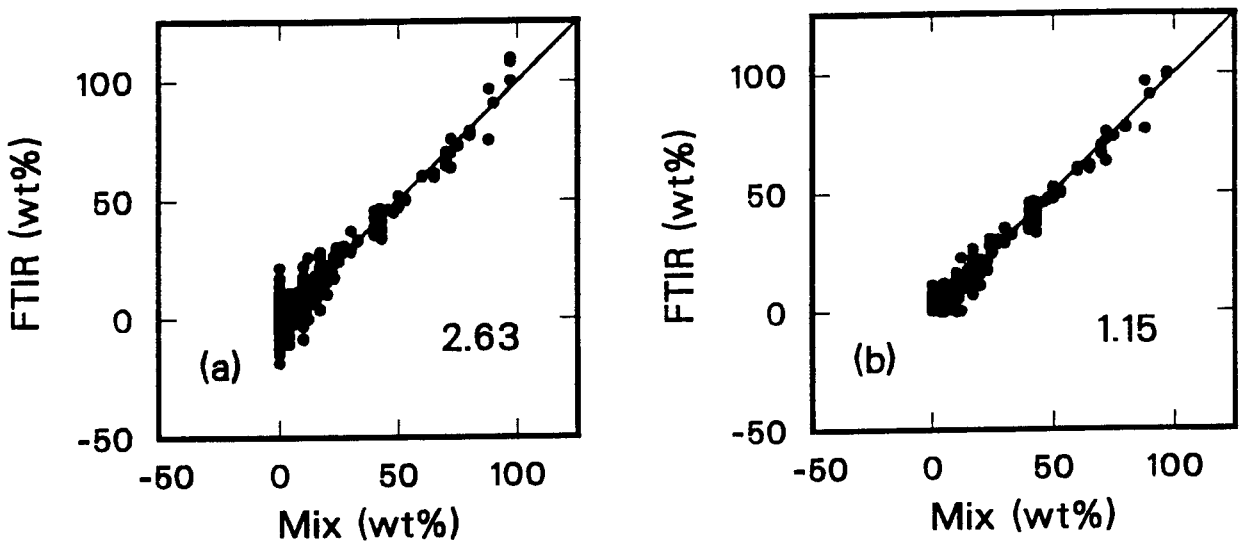

Fig. 3—Comparison of known and derived mineral concentrations for least-squares (a) and nonegative least-squares (b) programs. The average absolute difference between the known and the derived mineral concentrations for the 15 standards in the mixtures is plotted on each graph.

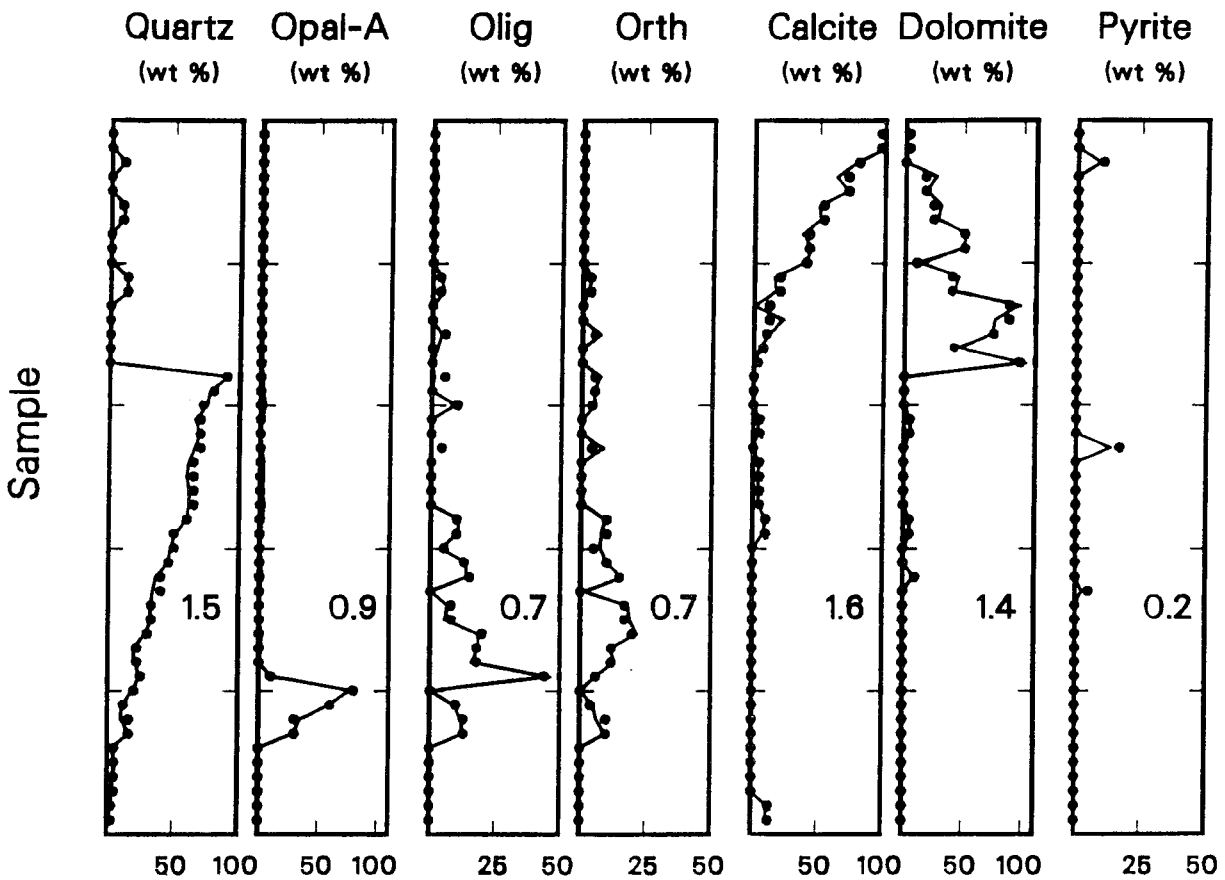

Fig. 4—Mineral concentration "logs" for quartz, opal-A, oligoclase, orthoclase, calcite, dolomite and pyrite (circles) compared to mineral concentrations determined from FTIR spectroscopy (solid line). The average absolute difference (includes zeros) between the ground truth and FTIR-determined concentration for each mineral is also plotted.

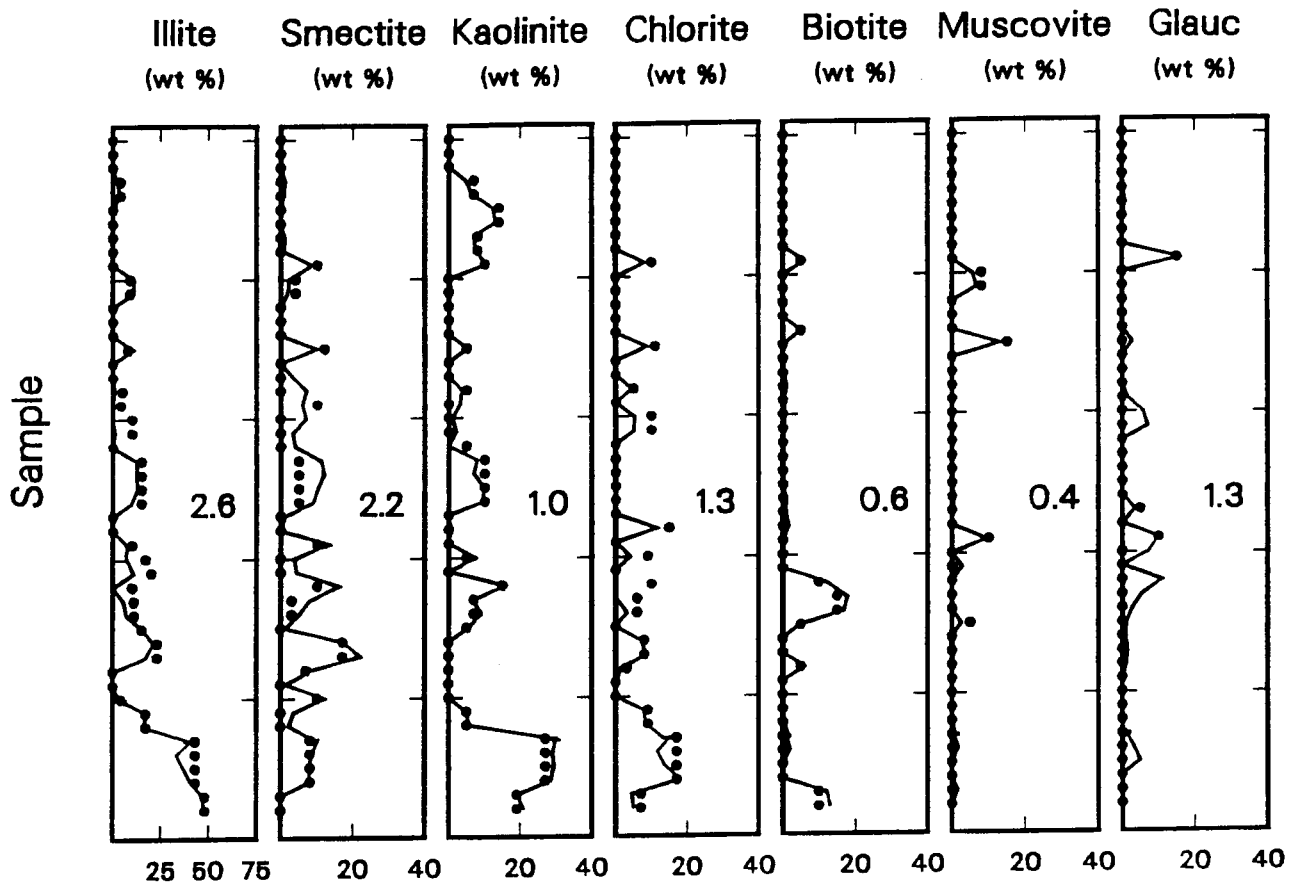

Fig. 5–Mineral concentration "logs" for illite, smectite, kaolinite, chlorite, biotite, muscovite and glauconite (circles) compared to mineral concentrations determined from FTIR spectroscopy (solid line). The average absolute difference (includes zeros) between the ground truth and FTIR-determined concentration for each mineral is also plotted.

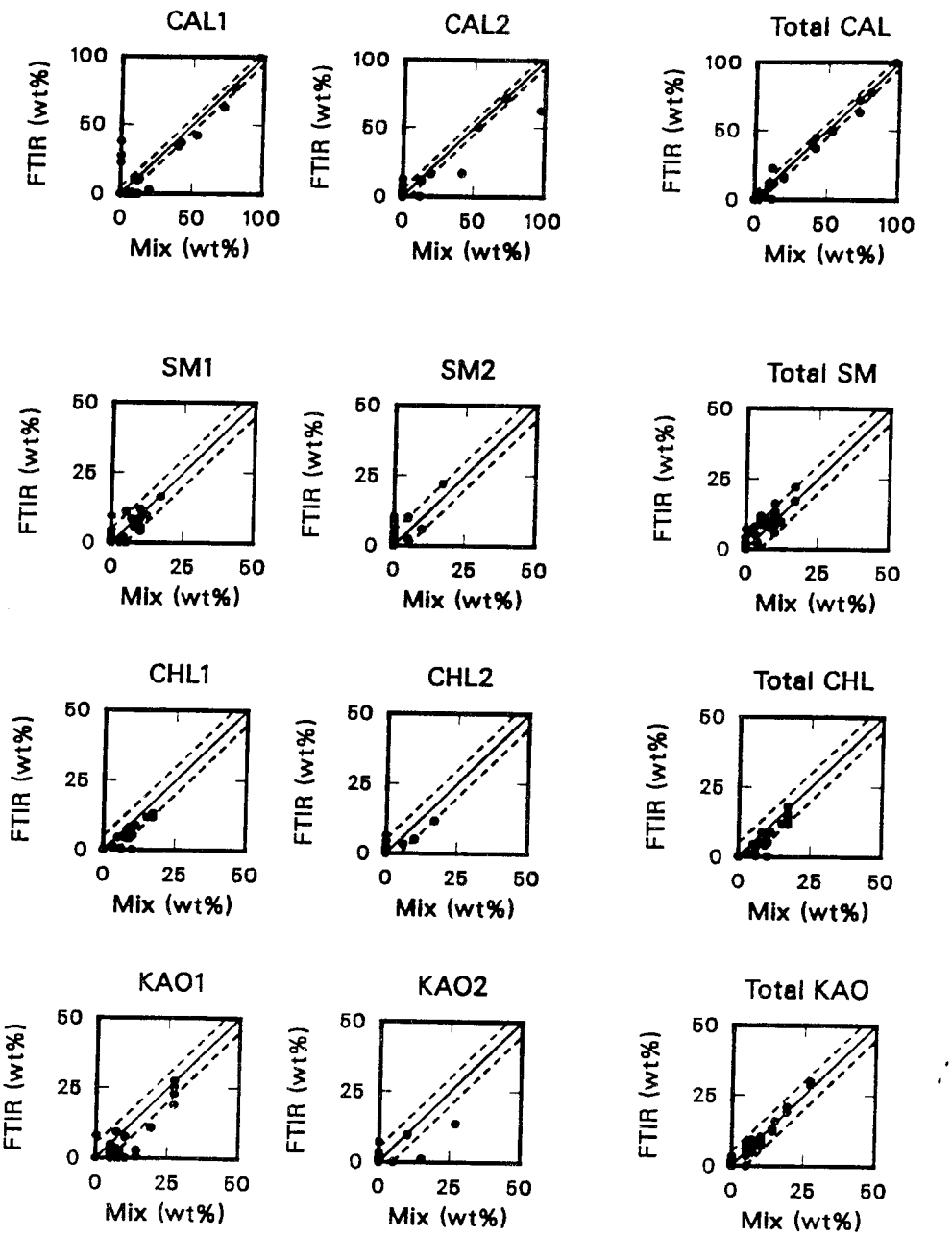

Fig. 6—Comparison of known and FTIR-derived mineral concentrations for CAL1, CAL2 and total calcite; SM1, SM2 and total smectite; CHL1, CHL2 and total chlorite; and KAO1, KAO2 and total kaolinite. The dashed lines represent the ±5 wt % error.